Effect of cysteamine hydrochloride-loaded liposomes on skin depigmenting and penetration

Carla Atallah, Celine Viennet, Sophie Robin, Sami Ibazizen, Hélène Greige-Gerges, Catherine Charcosset

HAL Id: hal-03759788
https://hal.science/hal-03759788

Submitted on 24 Aug 2022

Effect of cysteamine hydrochloride-loaded liposomes on skin depigmenting and penetration

Carla Atallah[a,b], Celine Viennet[c], Sophie Robin[d], Sami Ibazizen[d], Hélène Greige-Gerges[a], and Catherine Charcosset[b]

[a]*Bioactive Molecules Research Laboratory, Faculty of Sciences, Lebanese University, Lebanon.*

[b]*Laboratoire d'Automatique, de Génie des Procédés et de Génie Pharmaceutiques (LAGEPP), Université Claude Bernard Lyon 1, France.*

[c]*UMR 1098 RIGHT INSERM EFS BFC, DImaCell Imaging Ressource Center, University of Bourgogne Franche-Comté, Besançon, 25000, France*

[d]*Bioexigence SAS, Espace Lafayette, Besançon, France*

Abstract

Skin hyperpigmentation is caused by an excessive production of melanin. Cysteamine, an aminothiol compound physiologically synthetized in human body cells, is known as depigmenting agent. The aim of this study was to evaluate the depigmenting activity and skin penetration of liposome formulations encapsulating cysteamine hydrochloride. First, cysteamine hydrochloride-loaded liposomes were prepared and characterized for their size, polydispersity index, zeta potential and the encapsulation efficiency of the active molecule. The stability of cysteamine hydrochloride in the prepared liposome formulations in suspension and freeze-dried forms was then assessed. The *in vitro* cytotoxicity of cysteamine and cysteamine-loaded liposome suspensions (either original or freeze-dried) was evaluated in B16 murine melanoma cells. The measurement of melanin and tyrosinase activities was assessed after cells treatment with free and encapsulated cysteamine. The antioxidant activity of the free and encapsulated cysteamine was evaluated by the measurement of ROS formation in treated cells. The *ex vivo* human skin penetration study was also performed using Franz diffusion cell. The stability of cysteamine hydrochloride was improved after encapsulation in liposomal suspension. In addition, for the liposome re-suspended after freeze-drying, a significant increase of vesicle stability was observed. The free and the encapsulated cysteamine in suspension (either original or freeze-dried) did not show any cytotoxic effect, inhibited the melanin synthesis as well as the tyrosinase activity. An antioxidant activity was observed for the free and the encapsulated cysteamine hydrochloride. The encapsulation enhanced the skin penetration of cysteamine hydrochloride. The penetration of this molecule was better for the re-suspended freeze-dried form than the original liposomal suspension where the drug was found retained in the epidermis layer of the skin.

Keywords: Cysteamine hydrochloride, cystamine, cytotoxicity, liposome, melanin, skin penetration, tyrosinase.

1 Introduction

Many compounds such as hydroquinone, kojic acid, and arbutin are used to treat hyperpigmentation; however, their use was associated with cytotoxic effects (Ephrem et al., 2017; Rendon & Gaviria, 2005; Solano et al., 2006). Cysteamine (cyst), an aminiothiol synthetized by human body cells; and its disulfide form, cystamine, have shown to possess a depigmenting effect on black gold fish (Chavin & Schlesinger, 1966; Frenk et al., 1968). Besides, the application of cysteamine Cream® on the ear of black female guinea pigs demonstrated a high depigmenting effect (Hsu et al., 2013). A randomized, double-blind vehicle-controlled clinical trial was also conducted to evaluate the efficacy and safety of this cream to treat epidermal melasma; the treatment with cysteamine cream® decreased the content of melanin (Farshi et al., 2017; Mansouri et al., 2015). It was reported that the depigmenting action of cyst and cystamine is due to the inhibition of tyrosinase activity which is the enzyme that plays a crucial role in the melanogenesis. Unlike hydroquinone, cyst and cystamine mechanisms of action are a melanogenesis inhibition and not a melanocytotoxicity (Qiu et al., 2000). Qiu et al. reported that 100 µM of cyst inhibit 21% of melanin and 87% of tyrosinase while 50 µM of cystamine inhibit 5% of melanin and 89% of tyrosinase (Qiu et al., 2000). These molecules could also reduce the reactive oxygen species (ROS) generation and enhance the intracellular glutathione (Lee et al., 2017; Okamura et al., 2014; Ribeiro et al., 2013; Shin et al., 2011; Sun et al., 2010). The production of (ROS) was significantly suppressed by low dose of cyst on 1-methyl-4-phenyl-1,2,3,6-tetrahydropyridine-induced dopaminergic neurodegeneration mice (Sun et al., 2010). Cyst also inhibited tert-butyl hydroperoxide-induced ROS production in human corneal endothelial cells (Shin et al., 2011). It reduced ROS production by 33% in phorbol 12-myristate-13-acetate stimulated macrophages (Okamura et al., 2014). In addition, cyst inhibited vascular endothelial growth factor-induced ROS generation in a concentration-dependent manner, with maximum effect at 50 µM (Lee et al.,

64 2017). Moreover, cystamine decreased ROS levels evoked by H_2O_2 or staurosporine in mutant

65 cells (Ribeiro et al., 2013).

66 However, cyst presents an offensive odor and is unstable in solutions where it undergoes

67 oxidation to cystamine (Atallah, Charcosset, et al., 2020). The encapsulation of many skin

68 whitening agents in delivery systems improved their stability (Ephrem et al., 2017). Moreover,

69 it increased their concentration at the targeted site by improving skin permeation, penetration

70 or distribution (Ephrem et al., 2017). Liposomes are nanometric spherical vesicles able to

71 encapsulate hydrophilic, hydrophobic and amphiphilic molecules. They are biodegradable,

72 biocompatible and present a low toxicity (Zylberberg & Matosevic, 2016).

73 Cyst can be used in different forms such as cyst (base form), cyst hydrochloride (cyst HCl),

74 phosphocyst, and cyst bitartrate (**Figure 1**). An increase of the stability of the base form of cyst

75 was previously demonstrated after encapsulation in liposomes suspension (original and from

76 freeze-dried form) compared to free cyst (base form) during storage at 4°C (Atallah, Greige-

77 Gerges, et al., 2020). However, after 60 hours, the remaining cyst in liposome suspension was

78 very low. Therefore, cyst HCl was used in this study because the salt form of this molecule is

79 more stable than its base form (Wiedmann & Naqwi, 2016).

80 The aim of this study was to investigate the effect of cyst HCl-loaded liposomes on

81 melanogenesis and oxidative stress in cultured B16 cells. Skin penetration assays were also

82 conducted on *ex-vivo* human skin. Blank and cyst HCl-loaded liposomes were prepared by the

83 ethanol injection method and characterized for their size, polydispersity index and zeta

84 potential. The encapsulation efficiency of cyst HCl (EE%) in liposomes was also calculated.

85 The amount of residual ethanol in the blank liposomes was determined by NMR technique.

86 Blank and cyst HCl-loaded liposomes were freeze-dried according to the optimized protocol

87 previously described (Gharib et al., 2018). The lyophilized liposomes were then re-suspended

88 with ultra-pure water. The stability of free cysteamine dissolved in water and that of the cyst

89   HCl-loaded liposome suspensions (original or freeze-dried form) was evaluated at 4°C during

90   6 months. The cytotoxicity of free cyst HCl, cystamine and the suspensions of blank- and cyst

91   HCl-loaded liposomes (original or freeze-dried) were evaluated by MTT assay. In addition, the

92   effects of the same formulations on the *in vitro* melanin content and tyrosinase activity were

93   measured. Moreover, the antioxidant activity of the free and the encapsulated cyst HCl was

94   assessed by the measurement of ROS formation induced by the presence of H_2O_2 in B16 cells.

95   Finally, the skin penetration of free- and cyst HCl-loaded liposomes was compared using the

96   Franz diffusion cell.

2   Materials and Methods

2.1   Materials

Cyst HCl, cystamine dihydrochloride, metformin hydrochloride, (3-(4, 5-dimethylthiazol-2-yl)-2, 5-diphenyltetrazolium bromide), DMSO, L-DOPA and NaOH were purchased from Sigma-Aldrich (Buchs, Switzerland). Phospholipon 90H (90% soybean PC, 4% lysoPC, 2% triglycerides, 2% water, and 0.5% ethanol) was obtained from Lipoid GmbH (Ludwigshafen, Germany). Cholesterol was obtained from the Fisher chemical (Loughborough, UK). HP-β-CD-oral grade (MS=0.85) was purchased from Roquette (Lestrem, France). Sodium dodecyl phosphate and phosphoric acid were obtained from Sigma-Aldrich (China). (trimethylsilyl)-2,2,3,3-tetradeutepropropionic acid sodium salt, 2,7-dichlorodihydrofluorescein diacetate and H_2O_2 were purchased form Sigma-Aldrich (USA). Deuterium oxide (D_2O) was purchased from Acros organics (USA). Dulbecco's Modified Eagle Medium (DMEM), fetal bovine serum (FBS), penicillin, and streptomycin were purchased from Dominique Dutscher (France). All other chemicals were of analytical grade.

2.2   Cyst HCl-loaded liposomes suspensions preparation (original and re-suspended after freeze-drying)

Liposomes were prepared by ethanol injection method, as described by Sebaaly et al. (2016). The organic phase was prepared by dissolving phospholipon 90H (saturated lipid) (100 mg) and cholesterol (50 mg) in absolute ethanol (10 mL). Then, the organic phase was injected into the aqueous phase (20 mL) containing 5 mg/mL of cyst HCl, using a syringe pump (Fortuna optima, GmbH-Germany), at a temperature above the transition temperature of the phospholipid (55°C) and under magnetic stirring at 400 rpm. The contact between the organic solution and the aqueous phase leads to a spontaneous liposome formation. The liposomal suspensions were then left for 15 min at 25°C under stirring (400 rpm). The ethanol was removed by rotary evaporation (Heidolph GmbH, Germany) under reduced pressure at 40°C

6

122 and the obtained liposomal solutions were stored at 4°C. Each preparation was performed in

123 triplicate.

124 The freeze drying of blank- and cyst HCl-loaded liposomes was done as previously reported

125 (Atallah, Greige-Gerges, et al., 2020). In brief, blank liposomes and cyst HCl-loaded liposomes

126 (PH 90H: Chol: cyst molar ratios 1:0.98:10) were freshly prepared; 5 mL were then

127 ultracentrifuged at 170,000g for 1 h at 4 °C. The supernatant was removed, and the pellet was

128 re-dissolved in an aqueous solution of 50 mM HP-β-CD (2 mL). The samples were kept at −20

129 °C overnight then placed into the drying chamber of Cryonext 23,020 freeze-dryer (Trappes,

130 France), pre-cooled to -20°C, then lowered to -40°C with a slow cooling profile of 0.5°C/min.

131 The product was stabilized for 30 min at -38 °C before the vacuum was applied. Primary drying

132 was executed at a pressure of 150 μbar for 3 h at -10°C, then the temperature of the drying

133 chamber was progressively increased to 5 °C for 6 h at 250 μbar, to reach finally 10°C at 350

134 μbar for 9 h. A secondary drying step for 10 h at 20°C and 100 μbar pressure was applied.

135 Finally, the vials were removed from the freeze-dryer, closed with rubber caps, and stored at

136 4°C. The lyophilized liposomes were then re-suspended with ultra-pure water to the original

137 volume (5 mL).

138 **2.3   Cyst HCl-loaded liposomes characterization**

139 The size, polydispersity index and zeta potential were determined using Malvern Zetasizer

140 Nanoseries (Zetasizer Nano ZS; Malvern Instruments Ltd, France). All batches were diluted

141 with ultrapure water. The particle-size distribution data were collected using the DTS (nano)

142 software (version 5.10) provided with the instrument. Zeta potential was calculated using

143 Smoluchowski's equation from the electrophoretic mobility of liposomes. All measurements

144 were carried out at 25°C after 2 min of equilibration and were performed in triplicate. Data

145 were expressed as the mean values ± SD.

146   For the calculation of EE%, liposomal suspensions (5 mL) were ultra-centrifuged (OptimaTM

147   Ultracentrifuge, Beckman Coulter, USA) at 170,000g for 1 h at 4°C to separate the free cyst

148   HCl (supernatant) from the liposomes loading cyst HCl (pellet). The pellet was re-suspended

149   in water (5 mL). The total liposomal suspension as well as the re-suspended pellet were

150   sonicated and then analyzed by ion pair chromatography method as described below. This

151   allows to determine the total and encapsulated cyst HCl in the liposomal suspensions.

152   The encapsulation efficiency (EE %) of cyst HCl was calculated using the formula:

153
$$EE_{Cyst\ HCl}\% = \frac{[Cyst\ HCl]_{encapsulated}}{[Cyst\ HCl]_{total}} \times 100$$

154   Where $[Cyst\ HCl]_{encapsulated}$ and $[Cyst\ HCl]_{total}$ represent the concentration of encapsulated cyst

155   HCl (pellet) and the concentration of the total cyst HCl present in the liposomal suspension,

156   respectively.

157   **2.4   Cyst HCl and cystamine quantification**

158   To quantify cyst HCl and cystamine in the different formulations, an ion-pair chromatography

159   with an isocratic mode consisting of acetonitrile:water containing 0.1% phosphoric acid and

160   sodium dodecyl phosphate (4 mM) (v/v, 45:55) was used. The column was a reverse-phase

161   Kinetex C18 column (4.6 × 100 mm, 2.6 μm). 20 μL were injected in the column maintained at

162   25°C with a flow rate of 1.0 mL/min, and the detection wavelength was 215 nm. Metformin (1

163   μg/mL) was used as an internal standard. Linearity was between 2.5 and 100 μg/mL for cyst

164   HCl and between 5 and 100 μg/mL for cystamine. This method was previously used for the

165   quantification of cyst in its base form; the same chromatographic results were obtained as for

166   cyst HCl (retention time, limits of detection and quantification).

167   **2.5   Ethanol quantification in the blank liposomal suspension**

168   The quantity of ethanol present in the blank liposomal suspension was also determined by NMR

169   technique according to Zuriarrain et al. (Zuriarrain et al., 2015). Blank liposomal suspensions

170 were centrifuged for 10 min at 11200g. The residual ethanol is supposed to be present in the

171 upper phase. The internal standard used was (trimethylsilyl)-2,2,3,3-tetradeutepropropionic

172 acid sodium salt (TSP) $(CH_3)_3SiCD_2CD_2CO_2Na$. 10 mg of TSP was dissolved in 400 μL D_2O

173 and 300 μL of the supernatant of the liposomal suspension. The number of moles of ethanol is

174 calculated from the NMR spectrum using the following equation:

175
$$n_{EtOH} = \frac{H_{IS}}{H_{CH2}} \times n_{IS} \times \frac{I_{CH2}}{I_{IS}}$$

176 Where H_{IS} and H_{CH2} are the numbers of hydrogen atoms present in the internal standard

177 structure (equals to 9) and in CH_2 group of ethanol (equals to 2), n_{IS} is the number of moles of

178 the internal standard (equals to 5.78×10^{-5} mole) and I_{CH2} and I_{IS} are the integration of the CH_2

179 group of ethanol and the internal standard peaks.

180 To simplify, we replaced H_{IS}, H_{CH2} and n_{IS} by their values to obtain the following equation:

181
$$n_{EtOH \, (mole)} = 0.00026 \times \frac{I_{CH2}}{I_{IS}}$$

182 **2.6   Stability of free cyst HCl in solution, suspended cyst HCl-loaded liposomes**

183 **(original and freeze-dried)**

184 The stability of cyst HCl-loaded liposome was compared to that of free cyst HCl. The liposomal

185 suspension (5 mL) was centrifuged, the supernatant was eliminated, and the pellet was re-

186 suspended in water. The concentration of the encapsulated cyst HCl was determined after the

187 destruction of liposomes by sonication. A solution of cyst HCl with the same concentration of

188 the encapsulated cyst HCl was also prepared in water and stored at 4°C. After 6 months of

189 storage at 4 °C, the concentration of the remaining cyst HCl in free cyst HCl solution and the

190 suspensions of liposomes loading cyst HCl was determined. Also, after three months of storage

191 at 4 °C, freeze-dried liposomes were re-suspended in 5 mL water and the remaining cyst HCl

192 concentration was measured using ion-pair chromatography.

193 **2.7   Cell culture**

194 B16 murine melanoma cells (Elabscience, CliniSciences, Nanterre, France) were grown in

195 Dulbecco's Modified Eagle Medium (DMEM) supplemented with 10% heat-inactivated fetal

196 bovine serum (FBS), 100 U/mL penicillin, and 100 µg/mL streptomycin. Cells were maintained

197 in an incubator at 37 °C in a humidified 5% CO_2 atmosphere and passaged weekly using trypsin

198 0.05%/EDTA 0.02% in PBS to maintain the optimum conditions for exponential growth.

199 **2.8   Preparation of the formulations**

200 Different concentrations of cyst HCl and cystamine (50; 60; 100 and 500 µM) were prepared

201 in culture medium. Blank liposomes (original and re-suspended after freeze-drying) were

202 prepared between 0.1 to 5.7% v/v in culture medium to evaluate their cytotoxic effect. The

203 suspensions containing total cyst HCl-loaded liposome (encapsulated and non-encapsulated)

204 were centrifuged and the pellet was re-suspended to obtain the encapsulated cyst HCl-loaded

205 liposome. The total (present in the whole suspension) and the encapsulated cyst HCl-loaded

206 liposome were diluted in culture medium to obtain 0.1 and 2.8 v/v%, respectively. The freeze

207 dried cyst HCl-loaded liposomes were re-suspended in water and then diluted in culture

208 medium to obtain 5.7 v/v%. These dilutions were made to obtain the same concentration of cyst

209 HCl (60 µM) in all formulations. Kojic acid (700 µM) was prepared in water and used as

210 positive control.

211 **2.9   Cytotoxicity analysis**

212 B16 melanoma cell viability was determined by the (3-(4, 5-dimethylthiazol-2-yl)-2, 5-

213 diphenyltetrazolium bromide) MTT assay. Cells were seeded in 96-well microtiter plates at a

214 density of $6x10^3$ cells/well. After 24 h of incubation at 37°C in 5% CO_2, cells were treated with

215 100 µL of each formulation described in section 2.8. After 24 and 48 h of incubation with the

216 different formulations, the medium was removed, cells were washed twice and 100 µL of MTT

217 solution (0.5 mg/mL in medium) were added to each well. Cells were incubated for 4 h at 37°C

218 and the produced formazan salts were then dissolved in DMSO. Absorbance was measured at

219 571 nm by spectroscopy on a microplate reader (Thermo Scientific, Multiskan FC).

2.10 Melanin measurement

221 B16 cells were seeded at a density of 10×10^4 cells/well in 6-well plates. Plates were incubated

222 for 24 h at 37°C in 5% CO_2 before being treated with cyst HCl (60 µM), cystamine (60 µM),

223 kojic acid (700 µM), blank liposomes (original suspension and re-suspended freeze-dried form),

224 total cyst HCl-loaded liposome suspension, encapsulated cyst HCl-loaded liposome suspension

225 and suspended freeze-dried cyst HCl-loaded liposome. After 24 and 48 h, cells were collected

226 by scraping into ice-cold PBS and pelleted. Intracellular melanin was extracted by solubilizing

227 cell pellets in 1N NaOH containing 10% DMSO for 2 h at 80°C. The melanin content of cell

228 lysate supernatants was measured spectrophotometrically at an absorbance of 405 nm against a

229 standard curve of synthetic melanin. Intracellular melanin content was adjusted by the amount

230 of protein.

2.11 Tyrosinase activity assay

232 Intracellular tyrosinase activity was determined by measuring the rate of oxidation of L-DOPA

233 to DOPAchrome. B16 cells were seeded at a density of 10×10^4 cells/well in 6-well plates. After

234 24 h, 2 mL of cyst HCl (60 µM), cystamine (60 µM), kojic acid (700 µM), blank liposomes

235 (original suspension and re-suspended after freeze-drying), whole suspension of cyst HCl-

236 loaded liposome, suspended cyst HCl-loaded liposome (encapsulated) and suspended freeze-

237 dried cyst HCl-loaded liposome were added to cells. 48 and 72h post-treatment, cells were

238 harvested by scraping into ice-cold PBS and lysed at room temperature for 15 min with 0.5%

239 Triton X-100 in PBS. Lysed cell supernatants (100 µL) were mixed with 100 µL of freshly

240 prepared L-DOPA solution (0.1% in PBS). Following incubation at 37°C for 1 h, absorbance

241 was measured at 450 nm and compared with a standard curve using mushroom tyrosinase.

242 Tyrosinase activity was normalized to the amount of protein (determined using the Bradford

243 assay).

2.12 Reactive oxygen species content

245 Intracellular ROS production was detected using the oxidation-sensitive fluorescence dye 2,7-

246 dichlorodihydrofluorescein diacetate (DCFH-DA). Cells were seeded at a density of 6×10^3

247 cells/well in 96-well plates. After 24 h, they were firstly treated 2 times over a period of 72 h

248 with 100 µL of tested substances, and secondly treated with H_2O_2 (100 µM in culture medium)

249 for 6 h. Then DCFH-DA solution (1 µM in culture medium) was added to cells for 30 min at

250 37°C. Immediately after PBS washing, fluorescence was quantified using a

251 spectrofluorophotometer (BioTek, Synergy H1) with 495 nm excitation and 527 nm emission

252 filters. ROS were observed under an inverted fluorescence microscope (Olympus, DP50).

2.13 *Ex vivo* skin penetration study with Franz cell

254 *Ex vivo* percutaneous permeation of cyst HCl was performed on thawed skin from a female

255 caucasian donor. Skin was defatted using a scalpel and then dermatomed with a dermatome

256 (Zimmer Biomet Electric® Dermatome). Skin discs were realized using a circled cutter and the

257 thickness range was between 400 and 600 microns. Skin discs were mounted on a Franz cells

258 system (PermeGear). Franz cells were previously filled with receptor fluid (RF) consisting of

259 PBS-EDTA 0.1% at pH 7.4. Skin discs were equilibrated during 1 h before measurement of

260 TEWL (Trans Epidermal Water Loss) using a tewameter TM300 (MDD 4, Courage &

261 Khazaka). The tested formulations were cyst HCl solution, total and encapsulated cyst HCl-

262 loaded liposomes and resuspended freeze-dried cyst HCl-loaded liposomes. 1 mL of each

263 formulation diluted to obtain 1200µM of cyst HCl as a final concentration has been deposited

264 on the skin. RF was sampled at different time points 0, 1, 4, 18 and 24h. At 24 h, formulations

265 were removed and skin discs were washed with RF (1 mL). Skin compartments were separated

266 using forceps in order to obtain epidermis and dermis. Samples (Washing, Epidermis and

267 Dermis) were weighed and then the active ingredient was extracted in methanol:water

268 extraction solvent (50:50, v/v) after stirring during 24 h. Finally, extracts were quantified by

269 ion pair chromatography.

270 **2.14 Statistical analysis**

271 The differences between the treated and the control cells were calculated using ANOVA

272 (GraphPad Prism 9; GraphPad Software, San Diego, CA) with $p < 0.05$ defining statistical

273 significance.

3   Results and discussion

3.1   Characterization of cyst HCl-loaded liposomes

The sizes of the blank and cyst HCl-loaded liposomes were similar with 211 ± 8 nm and 217 ± 22 nm for blank and loaded liposomes, respectively. The polydispersity index was 0.2 ± 0.1 for the blank and cyst HCl-loaded liposomes indicating that the liposomal population was homogeneous. The zeta potential of the blank liposomes (-17.95 ± 4.0 mV) was increased after the addition of cyst HCl (-2.37 ± 0.7 mV). This result indicates the presence of an interaction between cyst HCl and the liposomal suspension. The EE% of the studied formulation was 3.74 ± 0.46 % which is lower than the EE% of cyst-loaded liposome (21 ± 5.0%) found in our previous work using the base form of cyst (Atallah, Greige-Gerges, et al., 2020). Cyst (base form) and cyst HCl differ by their aqueous solubility, pH of their aqueous solution, and their stability. The base form may interact with negatively charged phosphate of phospholipids leading to a greater encapsulation when compared with cyst HCl form.

The remaining percentage of ethanol in the liposomal suspension depended on the time of evaporation and the remaining volume of liposomal suspension. In fact, the percentage of the ethanol in the liposomal suspension increased with the increase of the final volume of liposomal suspension. The percentage of ethanol in all the studied conditions was less than 2.6% **(Table S1)**.

3.2   Stability of cyst HCl-loaded liposomes

The stability of cyst HCl-loaded liposomes and free cyst HCl prepared in water was assessed after storage at 4°C. The total degradation of free cyst HCl was obtained after 16 days, whereas a remaining cyst HCl percentage of 9.5% was obtained in the cyst HCl-loaded liposomes in suspension form after 6 months of storage at 4°C. The total concentration of cyst HCl in the resuspended freeze dried liposomes was determined after 3 months of storage at 4°C showing that the concentration of cyst HCl determined at time 0 was stable after 3 months of storage

14

299 **(Figure 2)**. The stability of cysteamine in its hydrochloride form was much better than in its

300 base form. For the same concentration of the free drug (200 µg/mL), cysteamine in its base

301 from was totally converted to cystamine after 15h of storage at 4°C (Atallah, Greige-Gerges, et

302 al., 2020) while cyst HCl was totally converted after 16 days of storage at 4°C. The

303 encapsulation of cyst HCl increased its stability in suspension form (total degradation after 6

304 months of storage) and for a longer time when the formulation was freeze-dried (no degradation

305 after 3 months of storage). The base form of cyst (200 µg/mL) was totally oxidized after 60 h

306 in the liposomal suspension and 4 months in the freeze-dried form (Atallah, Greige-Gerges, et

307 al., 2020).

308 **3.3 Cytotoxicity of blank liposomes (original suspension and suspended freeze-dried**

309 **form)**

310 The cytotoxicity of the blank liposomes in suspension and the suspended freeze-dried form was

311 evaluated by MTT assay on B16 murine melanoma cells after 24 and 48 h of incubation.

312 Following the ISO 10993-5 guideline, percentages of cell viability above 80% are considered

313 as non-cytotoxic. Blank liposomes in suspension form did not show any cytotoxic effect at the

314 various volume concentrations (0.1; 1; 2; 2.8 and 5% v/v) **(Table S2)**. 5% of H_2O/ethanol

315 solution decreased the cell viability to $83 \pm 0.1\%$. Suspended freeze-dried blank liposomes

316 showed a higher cytotoxicity than the liposomal suspension after 24 h of incubation. For 5%

317 (v/v), the cytotoxicity of blank liposomal suspension was $90 \pm 0.1\%$ while it was $75 \pm 0.1\%$ for

318 the suspended freeze-dried form **(Table S2)**. The cytotoxicity of the liposomes decreased after

319 48 h. The cytotoxicity observed is probably due to the presence of the HP-β-CD (used as a

320 cryoprotectant) in the freeze-dried vesicles (Hammoud et al., 2019).

321 **3.4 Cytotoxicity of free cyst HCl and cystamine**

322 The cytotoxicity of free cyst HCl and cystamine was for the first time evaluated on B16

323 melanoma cell line. Free cyst HCl and cystamine did not show any cytotoxicity between 50 and

15

324 100 µM (cell viability > 92%). However, cystamine showed a higher cytotoxicity than cyst HCl

325 at 500 µM; cell viability was decreased to $59 \pm 0.1\%$ and $26 \pm 0.1\%$ after 24h of 500 µM cyst

326 HCl and cystamine treatments, respectively **(Figure 3A)**. Similarly, Qiu et al. showed that

327 cystamine (50 to 100 µM) did not present any cytotoxic effect on MM418c5, MM96L and HeLa

328 cells after 6 days of treatment (Qiu et al., 2000). According to these results, cyst HCl at a

329 concentration of 60 µM was chosen for the next analysis.

330 **3.5 Cytotoxicity of cyst HCl-loaded liposomes**

331 The cytotoxicity of the total and encapsulated cyst HCl loaded liposomes was also evaluated

332 on B16 melanoma cells. Cell viability of the total and encapsulated cyst HCl-loaded liposomes

333 was $92 \pm 0.1\%$ and $95 \pm 0.1\%$, respectively, after 24 h of incubation. However, the suspended

334 freeze-dried form was more cytotoxic ($74 \pm 0.1\%$) than the liposomal suspension **(Figure 3B)**.

335 **3.6 Inhibition of melanin synthesis**

336 To study the effect of cyst HCl loaded liposomes on melanogenesis, we examined the level of

337 melanin produced in B16 cells after 2 treatments during 72 h of incubation with free cyst HCl

338 and cystamine (culture media as control), whole liposome suspension encapsulating cyst HCl

339 and cyst HCl-loaded liposome (original liposome suspension as control), and resuspended

340 freeze-dried cyst HCl-loaded liposome (resuspended freeze-dried liposome as control). Kojic

341 acid was used as a positive control.

342 For the same concentration of cyst HCl and cystamine (60 µM), cystamine was able to reduce

343 the melanin content in the cells ($33.0 \pm 13.0\%$) more than cyst HCl ($26.0 \pm 8.6\%$). Kojic acid

344 used as a reference presented a melanin inhibition of $36.0 \pm 9.1\%$. Suspended freeze-dried blank

345 liposome did not show any inhibition of melanin (data not shown). The inhibition of melanin

346 was lower for the encapsulated ($22.0 \pm 0.9\%$) form compared to the free form ($26.0 \pm 8.6\%$).

347 The suspended freeze-dried cyst HCl-loaded liposome ($23.5 \pm 6.3\%$) showed a better inhibition

348 of melanin than the original suspension **(Figure 4)**.

16

349 **3.7 Inhibition of tyrosinase activity**

350 The tyrosinase enzyme plays a crucial role in melanogenesis. Kojic acid (used as positive

351 control) showed a strong inhibition of the enzyme activity ($36.2 \pm 5.8\%$). Cystamine ($28.2 \pm$

352 12.2%) and cyst HCl ($26.8 \pm 5.5\%$) inhibited the tyrosinase activity. Therefore, melanogenesis

353 inhibition by cyst HCl and cystamine in B16 cells occurs via direct inhibition of tyrosinase

354 activity, as previously described by Qiu et al. The effect of the cyst HCl encapsulated in

355 liposomes on the inhibition of the tyrosinase activity was investigated. The encapsulation of

356 cyst HCl decreased its inhibition of tyrosinase activity effect ($26.8 \pm 5.5\%$ was inhibited in

357 presence of free cyst HCl while $19.6 \pm 4.4\%$ and $18.3 \pm 2.9\%$ was inhibited for the encapsulated

358 cyst HCl loaded liposome and resuspended freeze-dried cyst HCl-loaded, respectively) **(Figure**

359 **4)**.

360 To the best of our knowledge, one study investigated the depigmenting effect of cyst *in vitro*

361 using pigmented melanoma MM418c5 cells. It showed that 100 µM of cyst inhibit 21.0% of

362 melanin and 87.0% of tyrosinase while 50 µM of cystamine inhibit 5.0% of melanin and 89.0%

363 of tyrosinase (Qiu et al., 2000).

364 **Figure 5** shows the microscopic observation of the cells after 2 treatments during 72 h of

365 incubation with free, total and encapsulated cyst HCl-loaded liposome in suspension and

366 resuspended freeze-dried forms. It also shows the solubilized cell pellets of the different treated

367 cells. A whitening effect was observed for all the formulations in comparison with the control.

368 **3.8 Reactive oxygen species content**

369 Intracellular oxidative stress was measured by the DCFH-DA assay. The cleavage of two

370 acetate groups of DCFH-DA by esterase will lead to the formation of DCFH that can be

371 oxidized to a highly fluorescent compound DCF by intracellular ROS. Therefore, the

372 fluorescence intensity of DCF can directly reflect the level of ROS in the cell (Rhee et al.,

17

373   2010). Hydrogen peroxide (H_2O_2) is a well-known inducer of oxidative stress. To estimate the

374   effect of cyst HCl and its encapsulation on the intracellular production of ROS in cultured B16

375   cells, cells were pretreated 2 times over a period of 72 h with 60 μM of cyst HCl and cystamine;

376   total and encapsulated cyst HCl-loaded liposome in suspension and resuspended freeze-dried

377   forms, and then treated for 6 h with H_2O_2. The inhibited percentage of ROS formation was

378   43.4±10.3% and 38.6±9.8% in the presence of free cyst HCl and cystamine, respectively. This

379   percentage was slightly decreased after the encapsulation of cyst HCl where it was 35.4±10.1%

380   and 33.6±11.6% for the encapsulated cyst HCl in suspension and resuspended freeze dried

381   forms **(Figure 6)**. After, the addition of 60 μM cyst or cystamine to the B16 cells, a decrease in

382   ROS levels by a factor of 1.8 and 1.6, respectively, in comparison with the control was

383   observed. The addition of the encapsulated cyst HCl in suspension and resuspended freeze dried

384   forms also decreased the relative fluorescence by 1.4 and 1.5 times in comparison with the

385   control. **Figure 7** shows fluorescence microscopy images of B16 cells. A decrease of the

386   DCFH-DA fluorescence in all cultures treated with the formulations containing cyst HCl was

387   observed in comparison to the control.

388   **3.9   Skin penetration study**

389   The cumulative amounts of cyst HCl penetrating the skin and found in the receptor fluid from

390   each of the liposomal formulation and controls over 24 h are shown in **Figure 8**. The

391   encapsulation of cyst HCl in liposomes increased its penetration through the human skin. The

392   quantity of cyst HCl found in the fluid receptor after 24 h of deposition was increased by 2.9-;

393   3.5- and 3.5-fold for the total, encapsulated and lyophilized cyst HCl loaded liposomes,

394   respectively in comparison to the free drug in solution **(Figure 8)**. Cystamine did not penetrate

395   the skin since it was not found in the receptor fluid nor in the epidermis layer.

396   **Figure 9** shows the retention of cyst HCl in the epidermis when the drug was free or

397   encapsulated in liposomes in suspension or in resuspended freeze-dried forms. The highest

18

398 quantity of retained cyst HCl in the epidermis was found for the cyst HCl-loaded liposome in

399 the resuspended freeze-dried form (150 µg/cm^2). The presence of HP-β-CD could be the reason

400 behind the increase of cyst penetration in the resuspended freeze-dried form. The cyclodextrin

401 is known to be a penetration enhancer of the drug through the membranes (Loftsson &

402 Sigurdardóttir, 1996; Yan et al., 2014). α-Cyclodextrin demonstrated its ability to promote the

403 trans corneal diffusion of cyst (Pescina et al., 2016). A slight decrease of the retention of the

404 molecule in the epidermis was observed for cyst HCl encapsulated in liposome (120.0 µg/cm^2)

405 in comparison with the free drug (140.0 µg/cm^2) while a higher decrease was obtained for the

406 total cyst HCl loaded liposome (85.0 µg/cm^2). No trace of cystamine was found in the

407 epidermis.

4   Discussion

409 Liposomes represent the most studied system for drug delivery through the skin. These delivery

410 systems are used to enhance stability, skin penetration, depigmenting effect and antioxidant

411 activity of several compounds. For example, vitamin A demonstrated better stability when

412 loaded into liposomes compared to the free form during exposure to UV radiation (Arsić &

413 Vuleta, 1999). The encapsulation of curcumin in liposomes provided substantially more

414 protection than the encapsulation in CDs (Matloob et al., 2014). Amphotericin B liposome

415 formulations showed a higher stability (shelf life of 1 year) compared to the free drug (4 and

416 14 days) (Manosroi et al., 2004). The chemical stability of fasudil, an anti-vasospastic agent,

417 was also enhanced after its encapsulation (Ishida et al., 2002). In this article, the encapsulation

418 of cyst HCl in liposomes enhanced its stability; the total degradation of cyst HCl was obtained

419 after 16 days in aqueous medium, and lasted for 6 months for the liposomal suspension.

420 Moreover, cyst HCl loaded liposomes were stable during freeze-drying, and stability was

421 maintained after 3 months of storage.

422 In addition, the cream containing liposome-encapsulated 4-n-butylresorcinol and resveratrol

423 was shown to be effective and safe for the treatment of melasma. (Kwon et al., 2020). Aloe

424 Vera loaded into liposomes was proposed for melasma treatment and as an effective skin care

425 formulation especially for anti-aging and skin regeneration (Ghafarzadeh & Eatemadi, 2017).

426 In this study, the encapsulation of cyst HCl in liposomes showed a decrease of the depigmenting

427 effect that could be due to the entrapment of the drug in the liposomes aqueous compartment.

428 Hydroxytyrosol liposomes presented better DPPH radical scavenging activity than free

429 hydroxytyrosol, which could be due to the fact that hydroxytyrosol was encapsulated inside the

430 liposomes with a high encapsulation rate (Yuan et al., 2017). Stronger free radical scavenging

431 effect was obtained in Orthosiphon stamineus liposomes that in nonformulated extract (Yücel

432 & Şeker Karatoprak, 2017). No variation of the antioxidant activity was observed for the

433 hydrophilic Crithmum maritimum after its encapsulation in liposomes (Alemán et al., 2019).

434 Also, our results are in accordance with Aleman et al. where the antioxidant activity was slightly

435 decreased after encapsulation in liposomes.

436 Liposomes also showed an increase of skin penetration of entrapped and non-entrapped

437 hydrophilic substances into human skin. The penetration study of the liposomal formulation

438 containing encapsulated and non-encapsulated carboxyfluorescein exhibited maximum

439 deposition of this compound in the stratum corneum, whereas the liposomes containing just the

440 encapsulated carboxyfluorescein inside the liposomes showed a higher penetration into deeper

441 skin layers, such as the viable epidermis, and through the skin to the receiver compartment of

442 Franz diffusion cell (Verma et al., 2003). Another study showed that maximum idebenone

443 penetration in dermis was achieved by liposomes compared to leciplex and invasomes (Shah et

444 al., 2015). The skin penetration of itraconazole (ITZ) was studied using an aqueous solution of

445 ITZ, CD/ITZ inclusion complex, ITZ loaded liposomes and the CD/ITZ inclusion complex

446 loaded into liposomes. The complex improved slightly the drug penetration while ITZ-HP-β-

447   CD-loaded liposomes exhibited significant increase in ITZ skin deposition compared to

448   liposomes containing ITZ alone (Alomrani et al., 2014). Our results are in accordance with the

449   literature as an increase of the skin penetration was observed with cyst HCl encapsulation

450   especially the freeze dried form containing HP-β-CD.

451   In this study, phopsholipon 90H (PH90H) and cholesterol were chosen to prepare liposomes

452   encapsulating cyst HCl. Previous studies used PH90H liposomes to enhance the skin

453   penetration of drugs of various pharmacological classes, like methotrexate, idoxuridine and

454   acyclovir. It was shown that their dermal penetration was improved (Ita et al., 2010). Tarnowska

455   et al. also used PH90H liposomes to study the skin absorption of Mg^{2+} and Ca^{2+} from thermal

456   spring water, and showed that the suspension improved the skin absorption of Ca^{2+} (Tarnowska

457   et al., 2020). Beside, a mixture of PH90H and cholesterol was used for preparation of liposomes

458   encapsulating terbinafine HCl by the ethanol injection method. The cutaneous application of

459   this formulation prolonged the antifungal activity (Beeravelli et al., 2014). Similarly, a

460   liposomal formulation based on PH90H and cholesterol encapsulating nadifloxacin showed a

461   better penetration in deeper layers of skin, when compared with the free drug (Shiny et al.,

462   2016). In addition, saturated PH90H are in a gel like state on the skin, due to their melting

463   temperature Tm around 50°C (Dörfler & Brezesinski, 1983). A study successfully confirmed

464   that hydrogenated phospholipids penetrate into the strateum corneum, a high amount of the

465   lipid was found in the upper skin layers and a gradual decrease was noticed in the deeper layers

466   showing an accumulation of saturated phosphatidylcholine in upper epidermal layers

467   (Gutekunst et al., 2018).

468   Liposomes can be applied on the skin under different forms such as gel or cream. Topical gels

469   are commonly prescribed for skin diseases. The use of topical gels is convenient and could

470   provide a prolonged skin retention of the drug, which is beneficial for the treatment of skin

471   disease. Several studies used the liposomal gel for skin applications. For example, Wang et al.

472   used liposomal gel dual-loaded with all-trans retinoic acid and betamethasone for enhanced

473   therapeutic efficiency of psoriasis (Wang et al., 2020). The dermal delivery of nadifloxacin was

474   enhanced using liposomal gel (Shiny et al., 2016). In addition, liposomal gels were developed

475   for the topical delivery of anthralin (Fathalla et al., 2020).

5   Conclusion

The encapsulation of cyst HCl increased the stability of the molecule especially when the formulation was freeze-dried. The formulation was not cytotoxic with the chosen concentrations. Cyst HCl and cystamine showed an inhibition of melanin and tyrosinase activity but cystamine was not able to penetrate the skin layers. The encapsulation of cyst HCl decreased its inhibition of melanin and tyrosinase activity but increased its penetration in the skin and its retention in the epidermis. The encapsulation didn't affect the antioxidant activity observed for the free cyst HCl. These findings are important for further application of cyst HCl liposomal formulations as a depigmenting agent. In this study, the results of depigmenting and anti-oxidant activities are based on vitro assays, precisely 2D cultures of B16. The *B16 cell* line is a widely used *model* for skin whitening and pigmentation studies. But potentially 3D models where cells are embedded in complex environments offer a better model of the *in vivo* cell environment than traditional 2D culture.

Declaration of Competing Interest

The authors declare that they have no known competing financial interests or personal relationships that could have appeared to influence the work reported in this paper.

6   References

496   **6   References**

497

498   Alemán, A., Marín, D., Taladrid, D., Montero, P., & Carmen Gómez-Guillén, M. (2019).

499   Encapsulation of antioxidant sea fennel (Crithmum maritimum) aqueous and ethanolic

500   extracts in freeze-dried soy phosphatidylcholine liposomes. *Food Research*

501   *International (Ottawa, Ont.)*, *119*, 665–674.

502   https://doi.org/10.1016/j.foodres.2018.10.044

503   Alomrani, A. H., Shazly, G. A., Amara, A. A., & Badran, M. M. (2014). Itraconazole-

504   hydroxypropyl-β-cyclodextrin loaded deformable liposomes: In vitro skin penetration

505   studies and antifungal efficacy using Candida albicans as model. *Colloids and*

506   *Surfaces. B, Biointerfaces*, *121*, 74–81. https://doi.org/10.1016/j.colsurfb.2014.05.030

507   Arsić, I., & Vuleta, G. (1999). Influence of liposomes on the stability of vitamin a

508   incorporated in polyacrylate hydrogel. *International Journal of Cosmetic Science*,

509   *21*(4), 219–225. https://doi.org/10.1046/j.1467-2494.1999.181682.x

510   Atallah, C., Charcosset, C., & Greige-Gerges, H. (2020). Challenges for cysteamine

511   stabilization, quantification, and biological effects improvement. *Journal of*

512   *Pharmaceutical Analysis*, *10*(6), 499–516. https://doi.org/10.1016/j.jpha.2020.03.007

513   Atallah, C., Greige-Gerges, H., & Charcosset, C. (2020). Development of cysteamine loaded

514   liposomes in liquid and dried forms for improvement of cysteamine stability.

515   *International Journal of Pharmaceutics*, 119721.

516   https://doi.org/10.1016/j.ijpharm.2020.119721

517   Beeravelli, S., J. N., R. V., & K. V., R. M. (2014). Formulation, Characterization and ex vivo

518   Studies of Terbinafine HCl Liposomes for Cutaneous Delivery. *Current Drug*

519   *Delivery*, *11*(4), 521–530.

520   Chavin, W., & Schlesinger, W. (1966). Some potent melanin depigmentary agents in the

521   black goldfish. *Die Naturwissenschaften*, *53*(16), 413–414.

522   Dörfler, H.-D., & Brezesinski, G. (1983). Phasenumwandlungserscheinungen in

523   Lecithin/Wasser-Systemen. *Colloid and Polymer Science*, *261*(3), 286–292.

524   https://doi.org/10.1007/BF01469677

525   Ephrem, E., Elaissari, H., & Greige-Gerges, H. (2017). Improvement of skin whitening agents

526   efficiency through encapsulation: Current state of knowledge. *International Journal of*

527   *Pharmaceutics*, *526*(1–2), 50–68. https://doi.org/10.1016/j.ijpharm.2017.04.020

528   Farshi, S., Mansouri, P., & Kasraee, B. (2017). Efficacy of cysteamine cream in the treatment

529   of epidermal melasma, evaluating by Dermacatch as a new measurement method: A

530   randomized double blind placebo controlled study. *Journal of Dermatological*

531   *Treatment*, 1–8. https://doi.org/10.1080/09546634.2017.1351608

532   Fathalla, D., Youssef, E. M. K., & Soliman, G. M. (2020). Liposomal and Ethosomal Gels for

533   the Topical Delivery of Anthralin: Preparation, Comparative Evaluation and Clinical

534   Assessment in Psoriatic Patients. *Pharmaceutics*, *12*(5), 446.

535   https://doi.org/10.3390/pharmaceutics12050446

536   Frenk, E., Pathak, M. A., Szabó, G., & Fitzpatrick, T. B. (1968). Selective action of

537   mercaptoethylamines on melanocytes in mammalian skin: Experimental

538   depigmentation. *Archives of Dermatology*, *97*(4), 465–477.

539   Ghafarzadeh, M., & Eatemadi, A. (2017). Clinical efficacy of liposome-encapsulated Aloe

540   vera on melasma treatment during pregnancy. *Journal of Cosmetic and Laser*

541   *Therapy: Official Publication of the European Society for Laser Dermatology*, *19*(3),

542   181–187. https://doi.org/10.1080/14764172.2017.1279329

543   Gharib, R., Greige-Gerges, H., Fourmentin, S., & Charcosset, C. (2018). Hydroxypropyl-ß-

544   cyclodextrin as a membrane protectant during freeze-drying of hydrogenated and non-

545   hydrogenated liposomes and molecule-in-cyclodextrin-in- liposomes: Application to

546   trans-anethole. *Food Chemistry*, *267*, 67–74.

547   https://doi.org/10.1016/j.foodchem.2017.10.144

548 Gutekunst, D., Hoogevest, P., & Heidecke, C. (2018). *The effect of saturated phospholipids*

549   *on human skin assessed with shotgun lipidomic analysis.*

550 Hammoud, Z., Khreich, N., Auezova, L., Fourmentin, S., Elaissari, A., & Greige-Gerges, H.

551   (2019). Cyclodextrin-membrane interaction in drug delivery and membrane structure

552   maintenance. *International Journal of Pharmaceutics*, *564*, 59–76.

553   https://doi.org/10.1016/j.ijpharm.2019.03.063

554 Hsu, C., Mahdi, H. A., Pourahmadi, M., & Ahmadi, S. (2013). Cysteamine cream as a new

555   skin depigmenting product. *Journal of the American Academy of Dermatology*, *68*(4).

556   https://doi.org/10.1016/j.jaad.2012.12.781

557 Ishida, T., Takanashi, Y., Doi, H., Yamamoto, I., & Kiwada, H. (2002). Encapsulation of an

558   antivasospastic drug, fasudil, into liposomes, and in vitro stability of the fasudil-

559   loaded liposomes. *International Journal of Pharmaceutics*, *232*(1–2), 59–67.

560   https://doi.org/10.1016/s0378-5173(01)00896-1

561 Ita, K. B., Du Preez, J., du Plessis, J., Lane, M. E., & Hadgraft, J. (2010). Dermal delivery of

562   selected hydrophilic drugs from elastic liposomes: Effect of phospholipid formulation

563   and surfactants. *Journal of Pharmacy and Pharmacology*, *59*(9), 1215–1222.

564   https://doi.org/10.1211/jpp.59.9.0005

565 Kwon, S.-H., Yang, J. H., Shin, J.-W., Park, K.-C., Huh, C.-H., & Na, J.-I. (2020). Efficacy of

566   liposome-encapsulated 4-n-butylresorcinol and resveratrol cream in the treatment of

567   melasma. *Journal of Cosmetic Dermatology*, *19*(4), 891–895.

568   https://doi.org/10.1111/jocd.13080

569 Lee, Y.-J., Jung, S.-H., Hwang, J., Jeon, S., Han, E.-T., Park, W. S., Hong, S.-H., Kim, Y.-M.,

570   & Ha, K.-S. (2017). Cysteamine prevents vascular leakage through inhibiting

571   transglutaminase in diabetic retina. *Journal of Endocrinology*, *235*(1), 39–48.

572   https://doi.org/10.1530/JOE-17-0109

573 Loftsson, T., & Sigurdardóttir, A. M. (1996). Cyclodextrins as Skin Penetration Enhancers. In

574   J. Szejtli & L. Szente (Eds.), *Proceedings of the Eighth International Symposium on*

575   *Cyclodextrins* (pp. 403–406). Springer Netherlands. https://doi.org/10.1007/978-94-

576   011-5448-2_90

577 Manosroi, A., Kongkaneramit, L., & Manosroi, J. (2004). Stability and transdermal

578   absorption of topical amphotericin B liposome formulations. *International Journal of*

579   *Pharmaceutics*, *270*(1), 279–286. https://doi.org/10.1016/j.ijpharm.2003.10.031

580 Mansouri, P., Farshi, S., Hashemi, Z., & Kasraee, B. (2015). Evaluation of the efficacy of

581   cysteamine 5% cream in the treatment of epidermal melasma: A randomized double-

582   blind placebo-controlled trial. *The British Journal of Dermatology*, *173*(1), 209–217.

583   https://doi.org/10.1111/bjd.13424

584 Matloob, A. H., Mourtas, S., Klepetsanis, P., & Antimisiaris, S. G. (2014). Increasing the

585   stability of curcumin in serum with liposomes or hybrid drug-in-cyclodextrin-in-

586   liposome systems: A comparative study. *International Journal of Pharmaceutics*,

587   *476*(1–2), 108–115. https://doi.org/10.1016/j.ijpharm.2014.09.041

588 Okamura, D. M., Bahrami, N. M., Ren, S., Pasichnyk, K., Williams, J. M., Gangoiti, J. A.,

589   Lopez-Guisa, J. M., Yamaguchi, I., Barshop, B. A., Duffield, J. S., & Eddy, A. A.

590   (2014). Cysteamine Modulates Oxidative Stress and Blocks Myofibroblast Activity in

591   CKD. *Journal of the American Society of Nephrology : JASN*, *25*(1), 43–54.

592   https://doi.org/10.1681/ASN.2012090962

593   Pescina, S., Carra, F., Padula, C., Santi, P., & Nicoli, S. (2016). Effect of pH and penetration

594   enhancers on cysteamine stability and trans-corneal transport. *European Journal of*

595   *Pharmaceutics and Biopharmaceutics*, *107*, 171–179.

596   https://doi.org/10.1016/j.ejpb.2016.07.009

597   Qiu, L., Zhang, M., Sturm, R. A., Gardiner, B., Tonks, I., Kay, G., & Parsons, P. G. (2000).

598   Inhibition of melanin synthesis by cystamine in human melanoma cells. *The Journal*

599   *of Investigative Dermatology*, *114*(1), 21–27. https://doi.org/10.1046/j.1523-

600   1747.2000.00826.x

601   Rendon, M. I., & Gaviria, J. I. (2005). Review of Skin-Lightening Agents. *Dermatologic*

602   *Surgery*, *31*(s1), 886–890. https://doi.org/10.1111/j.1524-4725.2005.31736

603   Rhee, S. G., Chang, T.-S., Jeong, W., & Kang, D. (2010). Methods for detection and

604   measurement of hydrogen peroxide inside and outside of cells. *Molecules and Cells*,

605   *29*(6), 539–549. https://doi.org/10.1007/s10059-010-0082-3

606   Ribeiro, M., Silva, A. C., Rodrigues, J., Naia, L., & Rego, A. C. (2013). Oxidizing Effects of

607   Exogenous Stressors in Huntington's Disease Knock-in Striatal Cells—Protective

608   Effect of Cystamine and Creatine. *Toxicological Sciences*, *136*(2), 487–499.

609   https://doi.org/10.1093/toxsci/kft199

610   Shah, S. M., Ashtikar, M., Jain, A. S., Makhija, D. T., Nikam, Y., Gude, R. P., Steiniger, F.,

611   Jagtap, A. A., Nagarsenker, M. S., & Fahr, A. (2015). LeciPlex, invasomes, and

612   liposomes: A skin penetration study. *International Journal of Pharmaceutics*, *490*(1–

613   2), 391–403. https://doi.org/10.1016/j.ijpharm.2015.05.042

614   Shin, Y. J., Seo, J. M., Chung, T. Y., Hyon, J. Y., & Wee, W. R. (2011). Effect of Cysteamine

615   on Oxidative Stress-induced Cell Death of Human Corneal Endothelial Cells. *Current*

616   *Eye Research*, *36*(10), 910–917. https://doi.org/10.3109/02713683.2011.593726

Shiny, A., Toomu, M., & Dhurke, R. K. (2016). ENHANCED DERMAL DELIVERY OF NADIFLOXACIN USING LIPOSOMES. *International Journal of Applied Pharmaceutics*, 53–59. https://doi.org/10.22159/ijap.2016v8i4.14315

Solano, F., Briganti, S., Picardo, M., & Ghanem, G. (2006). Hypopigmenting agents: An updated review on biological, chemical and clinical aspects. *Pigment Cell Research*, *19*(6), 550–571. https://doi.org/10.1111/j.1600-0749.2006.00334.x

Sun, L., Xu, S., Zhou, M., Wang, C., Wu, Y., & Chan, P. (2010). Effects of cysteamine on MPTP-induced dopaminergic neurodegeneration in mice. *Brain Research*, *1335*, 74–82. https://doi.org/10.1016/j.brainres.2010.03.079

Tarnowska, M., Briançon, S., Azevedo, J. R. de, Chevalier, Y., Arquier, D., Barratier, C., & Bolzinger, M. (2020). The effect of vehicle on skin absorption of Mg2+ and Ca2+ from thermal spring water. *International Journal of Cosmetic Science*. https://doi.org/10.1111/ics.12607

Verma, D. D., Verma, S., Blume, G., & Fahr, A. (2003). Liposomes increase skin penetration of entrapped and non-entrapped hydrophilic substances into human skin: A skin penetration and confocal laser scanning microscopy study. *European Journal of Pharmaceutics and Biopharmaceutics*, *55*(3), 271–277. https://doi.org/10.1016/S0939-6411(03)00021-3

Wang, W., Shu, G., Lu, K., Xu, X., Sun, M., Qi, J., Huang, Q., Tan, W., & Du, Y. (2020). Flexible liposomal gel dual-loaded with all-trans retinoic acid and betamethasone for enhanced therapeutic efficiency of psoriasis. *Journal of Nanobiotechnology*, *18*(1), 80. https://doi.org/10.1186/s12951-020-00635-0

Wiedmann, T. S., & Naqwi, A. (2016). Pharmaceutical salts: Theory, use in solid dosage forms and in situ preparation in an aerosol. *Asian Journal of Pharmaceutical Sciences*, *11*(6), 722–734. https://doi.org/10.1016/j.ajps.2016.07.002

642 Yan, Y., Xing, J., Xu, W., Zhao, G., Dong, K., Zhang, L., & Wang, K. (2014).

643 Hydroxypropyl-β-cyclodextrin grafted polyethyleneimine used as transdermal

644 penetration enhancer of diclofenac sodium. *International Journal of Pharmaceutics*,

645 *474*(1–2), 182–192. https://doi.org/10.1016/j.ijpharm.2014.08.021

646 Yuan, J.-J., Qin, F. G. F., Tu, J.-L., & Li, B. (2017). Preparation, Characterization, and

647 Antioxidant Activity Evaluation of Liposomes Containing Water-Soluble

648 Hydroxytyrosol from Olive. *Molecules*, *22*(6), 870.

649 https://doi.org/10.3390/molecules22060870

650 Yücel, Ç., & Şeker Karatoprak, G. (2017). Development and evaluation of the antioxidant

651 activity of liposomes and nanospheres containing rosmarinic acid. *Farmacia*, *65*.

652 Zuriarrain, A., Zuriarrain, J., Villar, M., & Berregi, I. (2015). Quantitative determination of

653 ethanol in cider by 1H NMR spectrometry. *Food Control*, *50*, 758–762.

654 https://doi.org/10.1016/j.foodcont.2014.10.024

655 Zylberberg, C., & Matosevic, S. (2016). Pharmaceutical liposomal drug delivery: A review of

656 new delivery systems and a look at the regulatory landscape. *Drug Delivery*, *23*(9),

657 3319–3329. https://doi.org/10.1080/10717544.2016.1177136

658

659

660

661 **Figure legends**

662 **Figure 1:** The structure of the different forms of cyst.

663 **Figure 2:** Stability study at 4°C of free cyst HCl, suspended cyst HCl-loaded liposome, and
664 freeze dried form of cyst HCl-loaded liposome suspended in water the day of HPLC analysis.

665 **Figure 3:** Cell viability of B16 melanoma cells in presence of different concentrations of cyst
666 HCl and cystamine (A) and in presence of free, total and encapsulated cyst HCl-loaded
667 liposome in suspension and resuspended freeze-dried form (B). Data are presented as means ±
668 SD (n = 6).

669 **Figure 4:** Inhibition percentages of melanin (A) and tyrosinase (B) for cyst HCl, cystamine,
670 kojic acid, total and encapsulated cyst HCl-loaded liposome in suspension and resuspended
671 freeze-dried forms after 2 treatments in 72 h incubation time. Data are presented as means ±
672 SD (n = 6). Statistical analysis was performed using ANOVA test; ns: not significant, *$p < 0.05$,
673 **$p<0.01$, ***$p < 0.001$, ****$p < 0.0001$.

674 **Figure 5:** Microscopic observations of cells after 72 h of incubation with the different
675 formulations (2 treatments) and representative image of the different solubilized pellets
676 obtained ((1)Total cyst HCl loaded liposome (2) Encapsulated cyst HCl loaded liposome (3)
677 Resuspended freeze-dried cyst HCl loaded liposome (4) Cyst HCl (5) Cystamine (6) Kojic acid)

678 **Figure 6**: Intracellular ROS formation measured by relative DCFH-DA fluorescence in
679 cultured B16 pretreated by H_2O_2 and treated with 60 μM of cyst HCl and cystamine; total and
680 encapsulated cyst HCl-loaded liposome in suspension and resuspended freeze-dried forms. The
681 formation of ROS was assayed by measuring the fluorescence of DCFH-DA. Data are presented
682 as means ± SD (n = 6). Statistical analysis was performed using ANOVA test; ***$p < 0.001$,
683 ****$p < 0.0001$.
684 **Figure 7:** Fluorescence microscopy images of B16 cells pretreated with H_2O_2 and treated for
685 72 h with free and encapsulated cyst HCl and cystamine.
686 **Figure 8:** Skin permeation profile of free and cyst HCl loaded liposome in suspension and
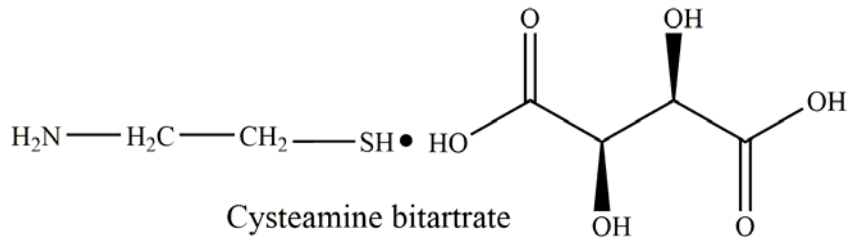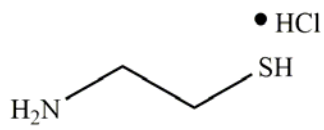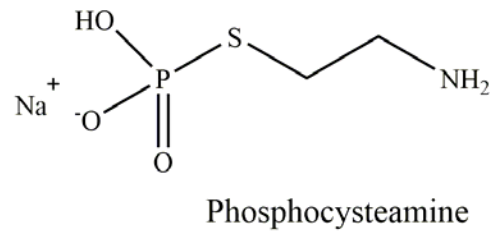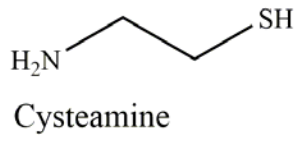687 resuspended freeze-dried forms.

688 **Figure 9:** Cyst HCl retention in the epidermis for the free, total and encapsulated cyst HCl-
689 loaded liposome in suspension and resuspended freeze-dried forms.

690

691   Figure 1

692

Cysteamine

Phosphocysteamine

Cysteamine hydrochloride

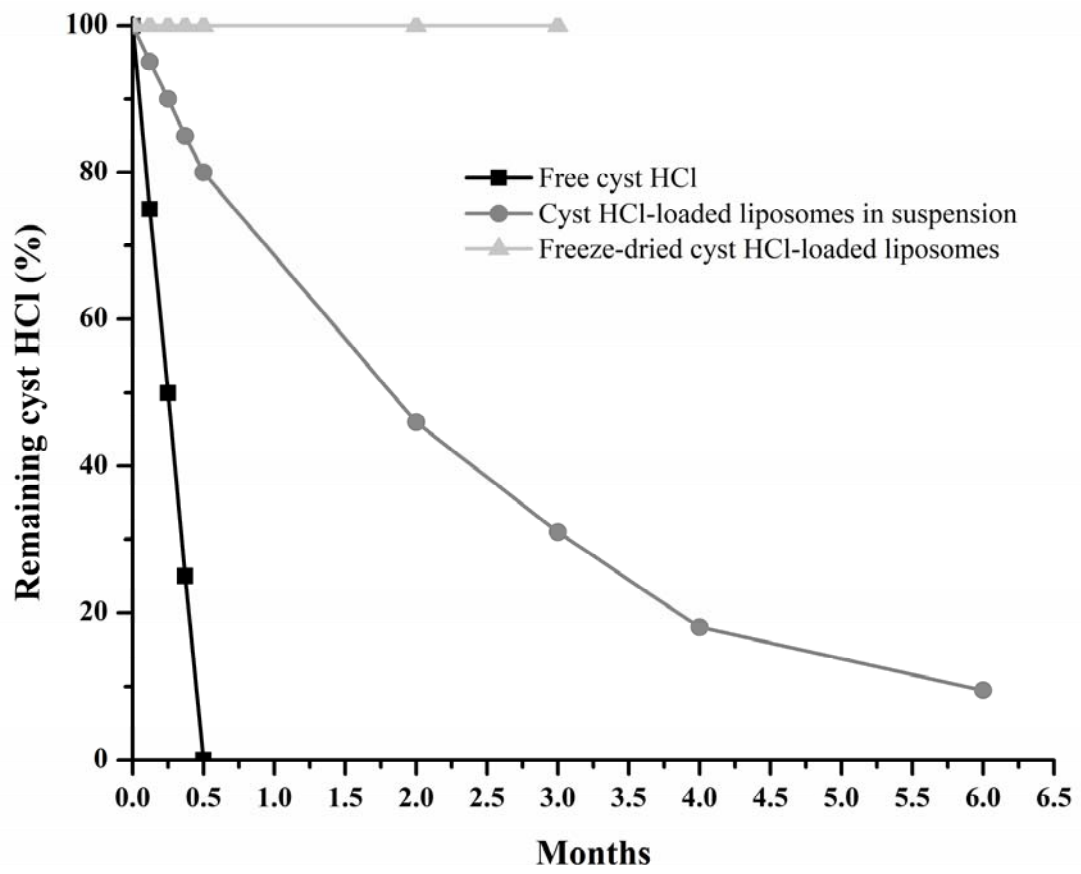Cysteamine bitartrate

693

694

695

696

697   Figure 2

698

699
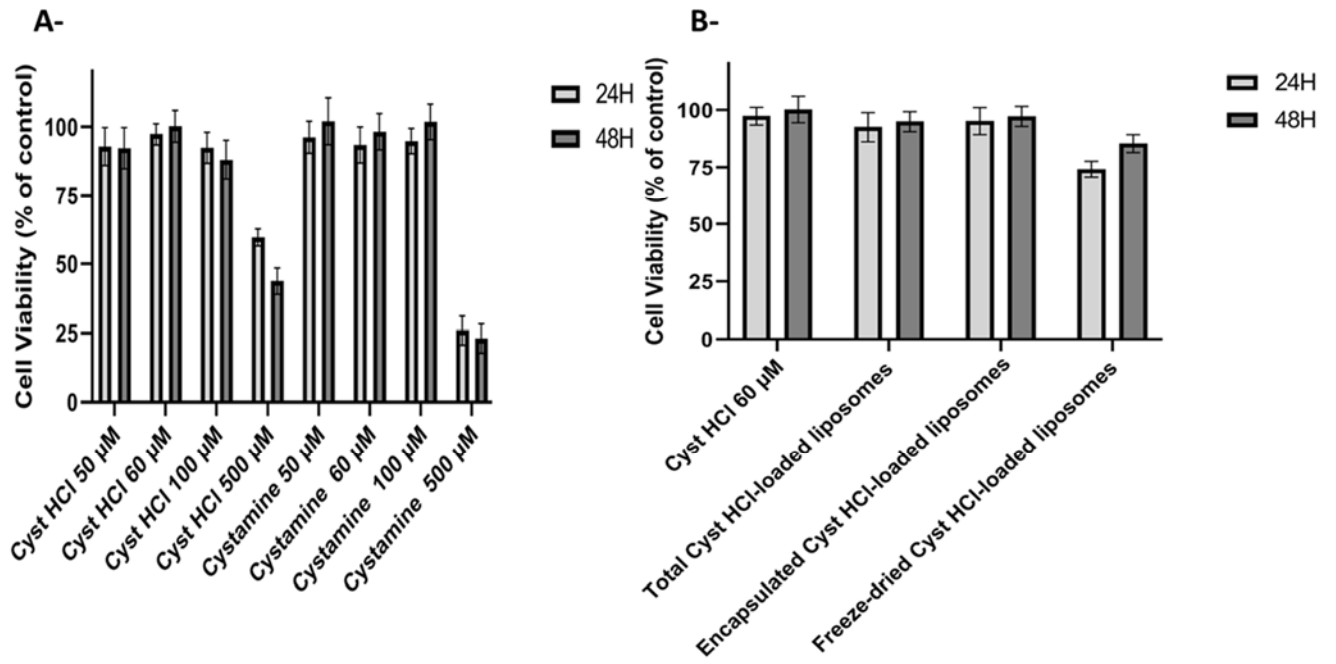
700

701

702

703   Figure 3
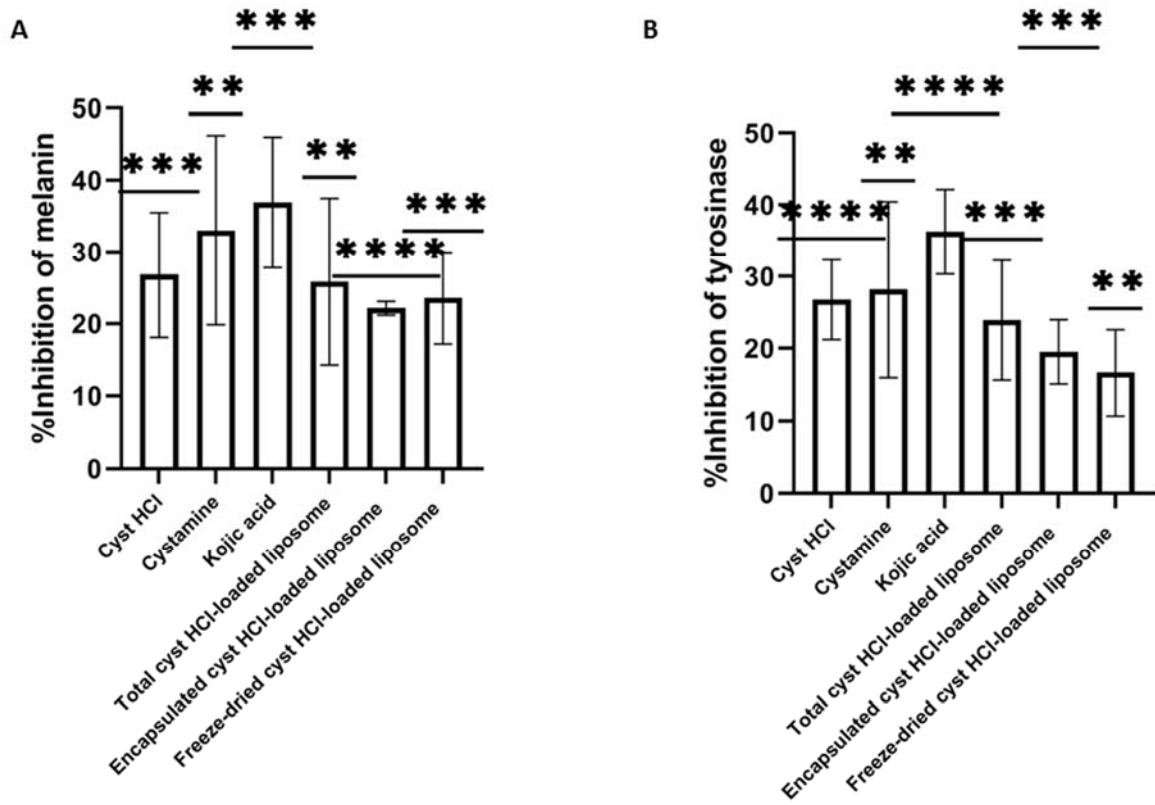
704

705

706

707

708

709   Figure 4

710

711

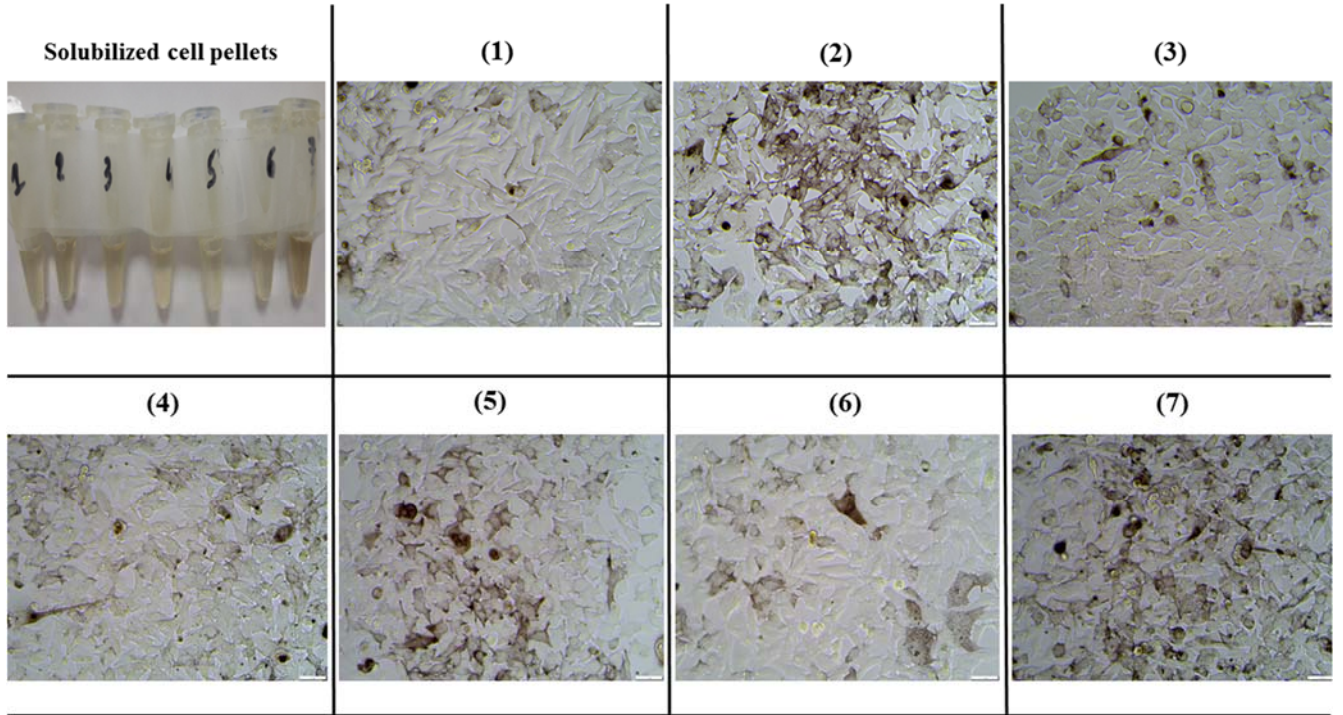712

713

714   Figure 5

715

716

717

718

719

720

721   Figure 6

722
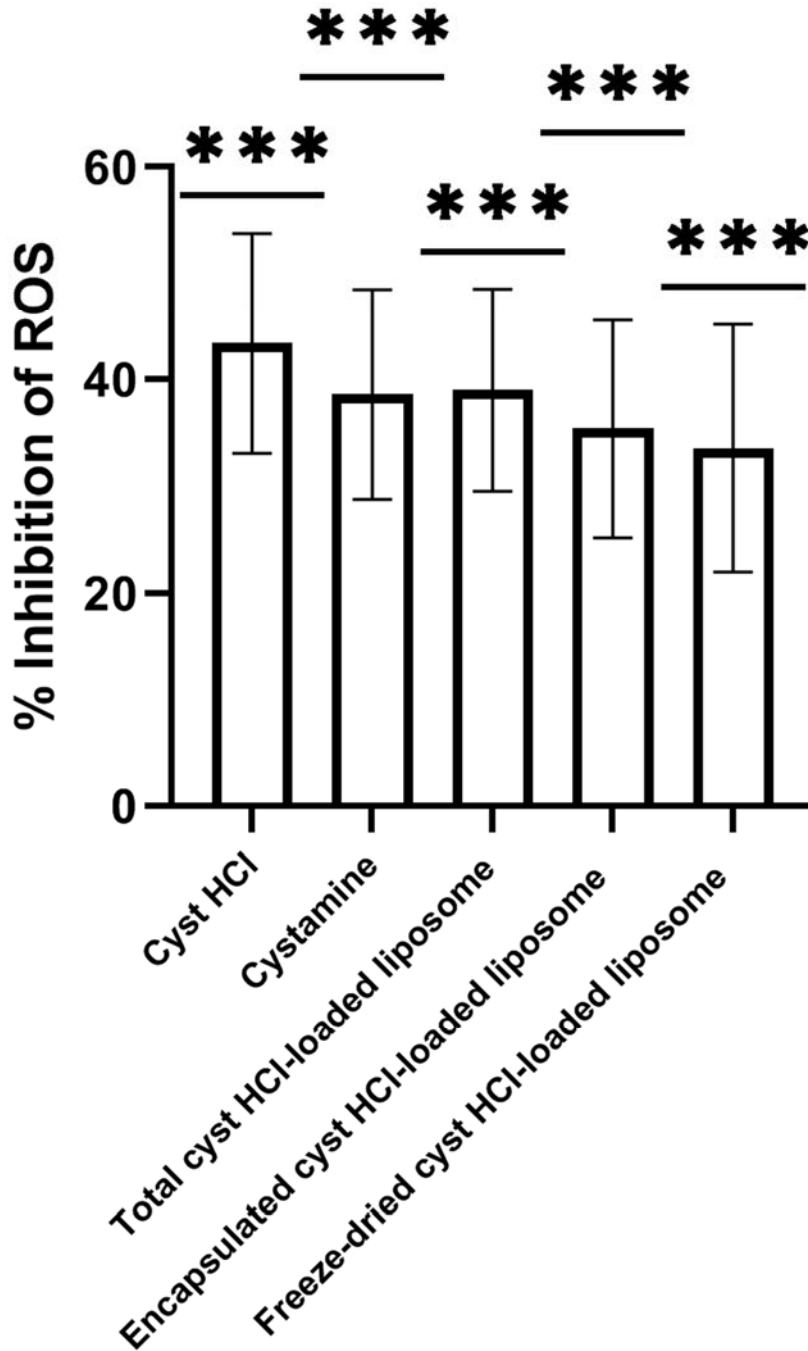
723

724

725

726   Figure 7

727

With H$_2$O$_2$

Total cyst HCl loaded liposome	Encapsulated cyst HCl loaded liposome	Resuspended freeze-dried cyst HCl loaded liposome

Control without H$_2$O$_2$

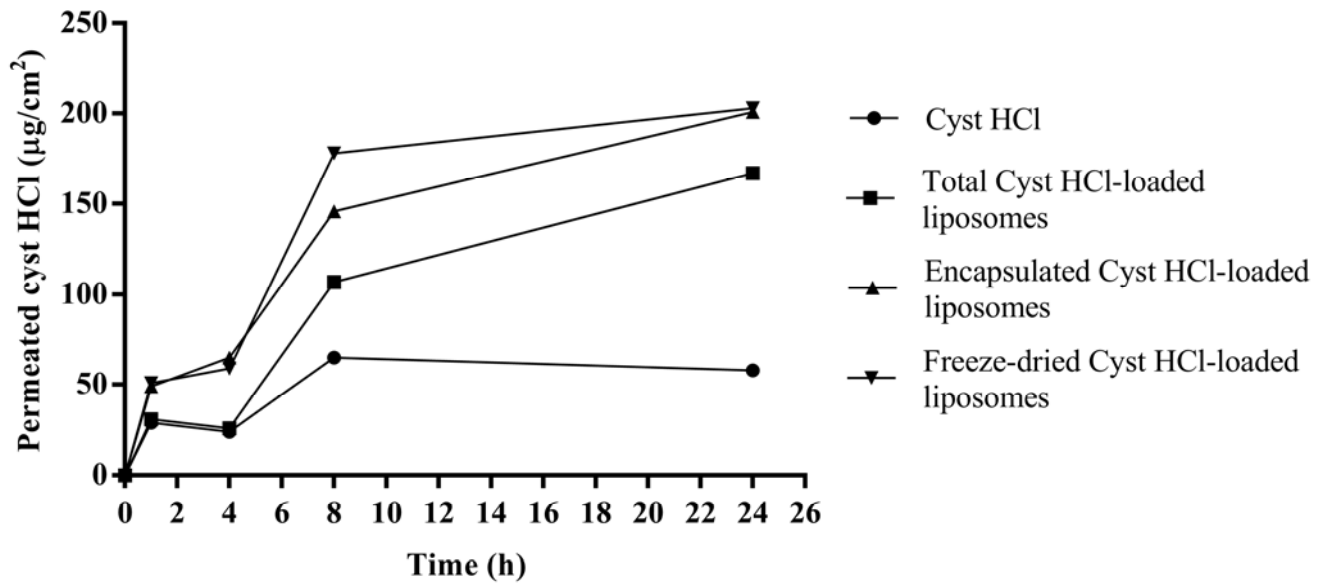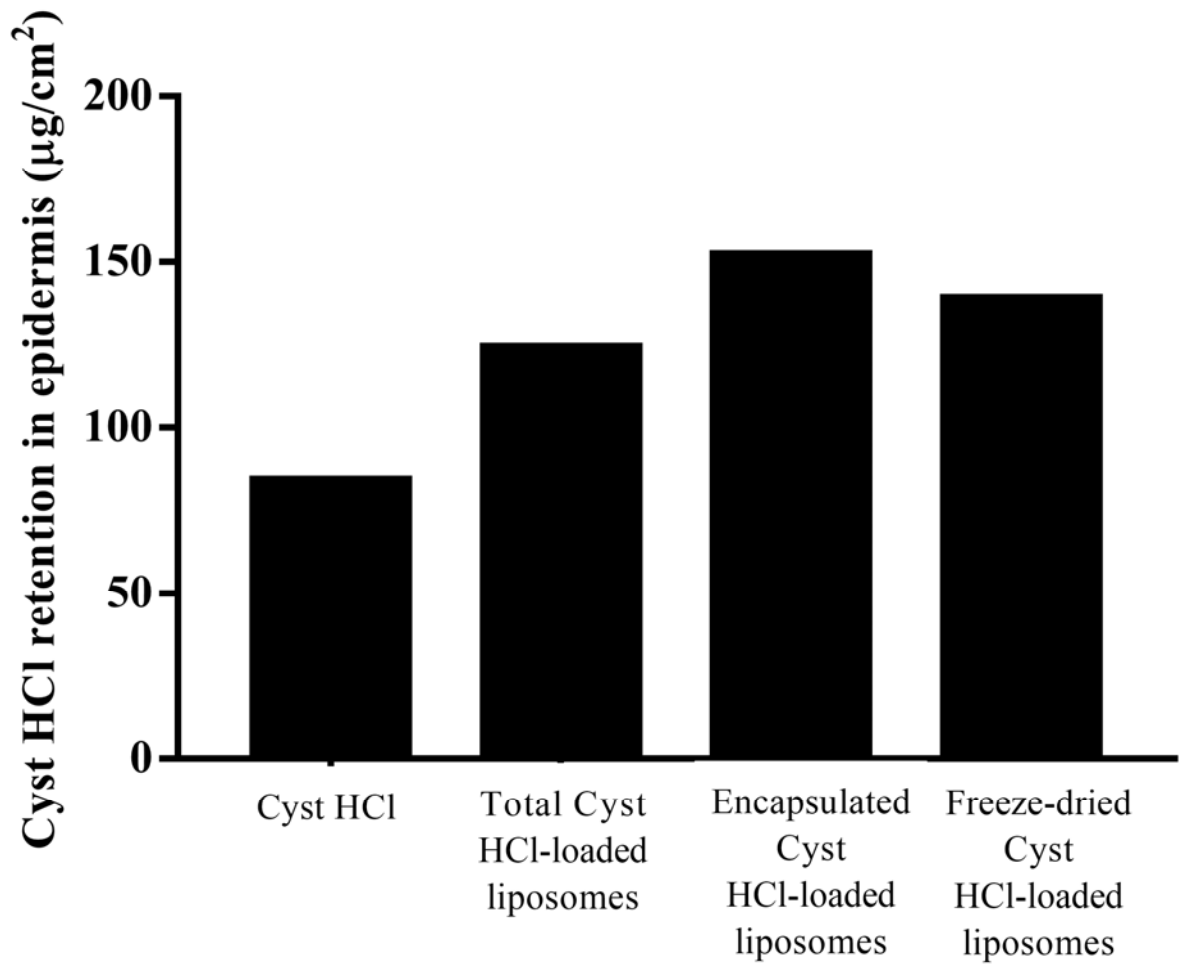|		
Cyst HCl 60 μM	Cystamine 60 μM	Control
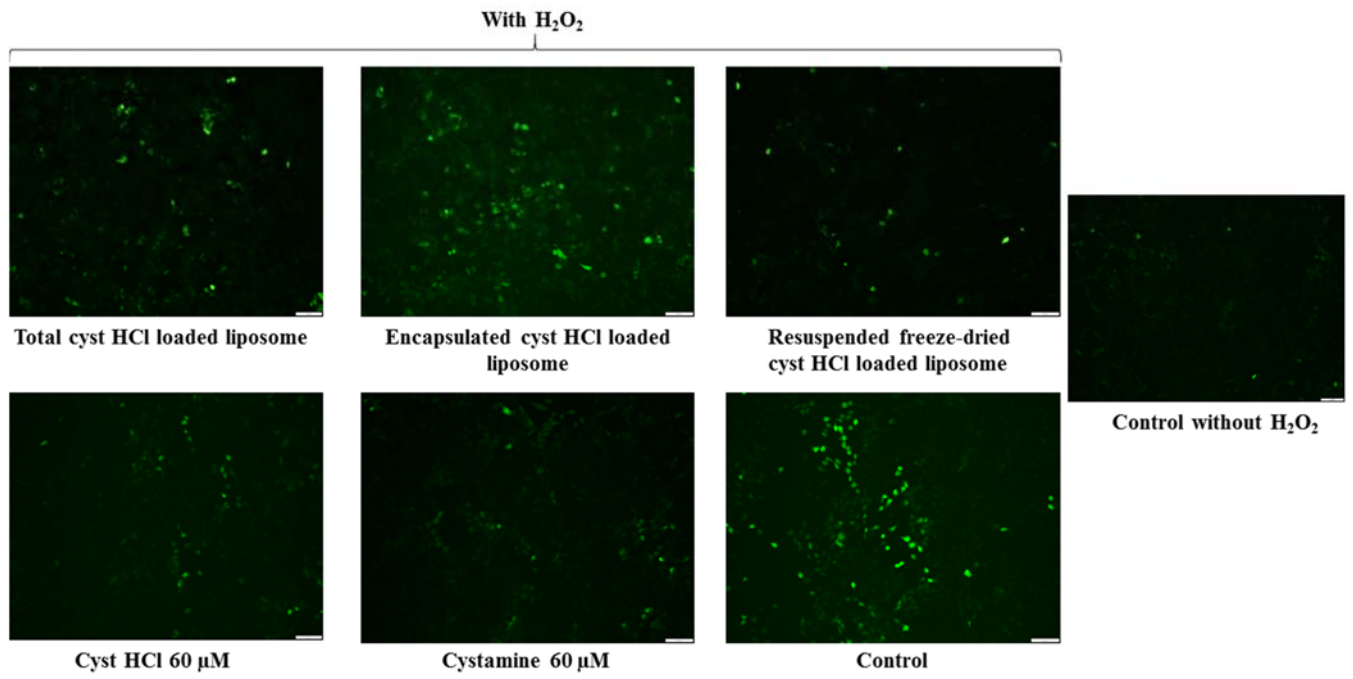
728

729

730

731   Figure 8

732

733

734

735

736

737   Figure 9

738

739

740

741

742